

Architecture, Engineering and Construction

BENDING BEHAVIOUR OF LAMINATED *Guadua* BAMBOO

Caori Takeuchi, *Ph.D.*

Professor, Universidad Nacional de Colombia, Bogotá, Colombia

Research Group: Análisis, Diseño y Materiales GIES

cptakeuchi@unal.edu.co

Dorian Linero, *Ph.D.*

Professor, Universidad Nacional de Colombia, Bogotá, Colombia

Research Group: Análisis, Diseño y Materiales GIES

dllineros@unal.edu.co

Abstract

This paper describes the flexural behaviour of Laminated *Guadua* Bamboo LGB. To elaborate the LGB, first, slats were glued together side by side to make boards and then, the boards were glued face to face to make the blocks from where the test pieces were cut. Samples of a square section with two different lengths were tested, expecting and obtaining failure by bending in the case of long samples and failure by shear in the case of short samples. In this research, the shear modulus and maximum shear stress in short samples and the modulus of elasticity and the flexural strength in the long samples were found. For each length, the orientation of the boards (and the slats) changed in two types of test. It was found that the values of stresses and modulus of elasticity depend on the orientation of the slats. In short samples, the average value of the maximum shear stress reached 6.2MPa when the normal stresses due to bending were parallel to the plane of the boards and 8.2MPa when they were perpendicular. The average value of the shear modulus was 307MPa when the normal stresses were parallel to the plane of the boards and 541MPa when they were perpendicular. In the case of long samples, the average value of the longitudinal modulus of elasticity was 23,050MPa when the normal stresses were parallel to the plane of the boards and 23,674MPa when they were perpendicular. The average value of the flexural strength was 94MPa when the normal stresses were parallel to the plane of the boards and 103MPa when they were perpendicular. The fissures propagate by changing their trajectory and avoiding crossing the fibres.

Keywords: Laminated *Guadua* bamboo, shear maximum stress; flexural strength; shear modulus; modulus of elasticity

Introduction

In Colombia, *Guadua angustifolia* Kunth bamboo has been used for many years in construction as main material of '*Bahareque encementado*' houses, which have a structural system of load-bearing walls built with a wood or bamboo framework covered by mortar applied on a mat of bamboo or '*esterilla*' (opened flat bamboo). In this country, *Guadua* is also used in its natural form (round *guadua*) as structural element of roofs, bridges and houses. Its design is currently normalised in the Colombian building Standards (AIS 2010).

However, the particularities of *Guadua* bamboo make difficult its use in construction. One of the reasons is that its physical and mechanical properties have high variability, since they depend on its growing conditions as height above sea level, environmental and topographic characteristics and the soil

properties among others (Correal and Arbeláez 2010; González et al. 2006; Osorio et al. 2005; Osorio et al. 2007; González and Leguizamón 2012). Another reason is that the connection between circular elements is difficult especially when the cross section is not constant.

The transformation of *Guadua* into a Laminated *Guadua* Bamboo LGB could increase and facilitate its use because it is possible to manufacture elements as beams and columns through an industrialized process controlling their dimensions. With a material of these characteristics, it is possible to have a complete production line that includes the processing of the material, the manufacture of structural elements and the prior preparation of the connexions between elements. Besides, the controlled manufacturing process could reduce the variability of the mechanical properties of the material. For this reason, it is important to know its mechanical behaviour. Recently, different investigations on the LGB mechanical behaviour have been developed (Correal and Ramírez 2010; Correal et al. 2014; Cortés et al. 2010; Cortés 2009; González et al. 2008a, González et al. 2008b, López and Correal 2009, Hackmayer et al. 2010), however, it is important to know more about the elastic and inelastic bending behaviour and determine the resistance values and elastic constants.

MATERIALS AND METHODS

Bending samples were obtained from blocks of LGB. To manufacture the LGB, strips were obtained from raw bamboo and transformed into slats. There were two steps of pressing. In the first step, slats were glued together side by side to make boards and, in the second step, the boards were glued face to face to make LGB blocks (Figure 1).

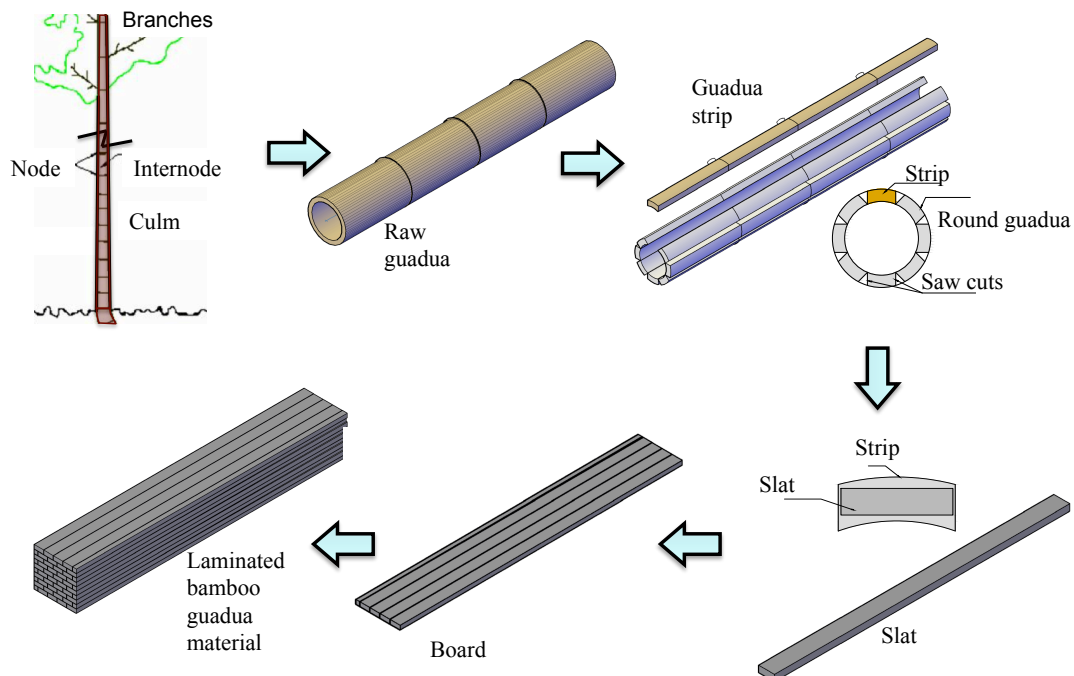


Figure 1. Manufacture of LGB blocks

A total of 10 blocks of 120cm length, 11cm width and a minimum height of 11.5cm were manufactured. To facilitate the identification of each type of samples, the coordinate system is shown in Figure 2. Direction 1 is parallel to the fibres and plane 2-3 illustrates the cross section. Axis 2 is perpendicular to

the boards and axis 3, parallel to the boards.

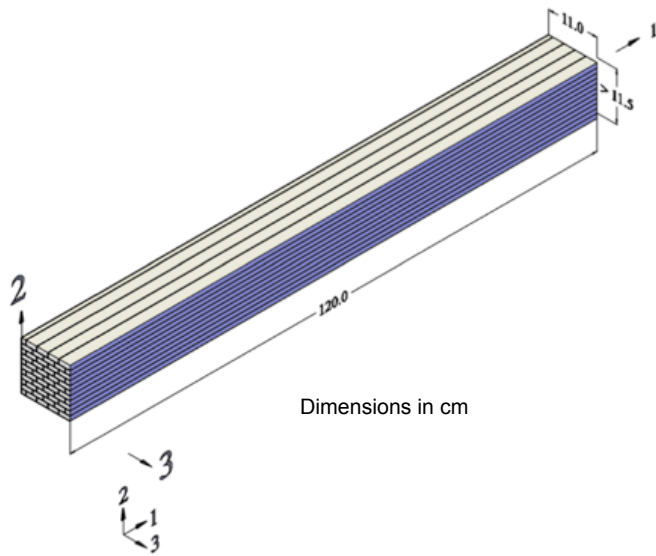


Figure 2. Coordinate system for LGB blocks

With the aim to obtain failure by bending and failure by shear, there were two lengths of samples. Additionally, in order to study the influence of the orientation of the boards (and the slats), the samples were tested in two different ways. For each length and each orientation of the slats, 10 samples were tested. In total, the number of tests was 40.

The samples were labelled with a number corresponding to the block of LGB from where they were cut. Letter F and numbers 11 indicate that the samples were requested to bending with normal stresses parallel to the fibre. Additionally, the samples had the letter "c" or "L", for short or long samples, respectively, and the letters "a" or "b", to indicate the orientation of the slats (Figure 3). All the samples had a square section of 4cm side and were tested with two symmetrical loads.

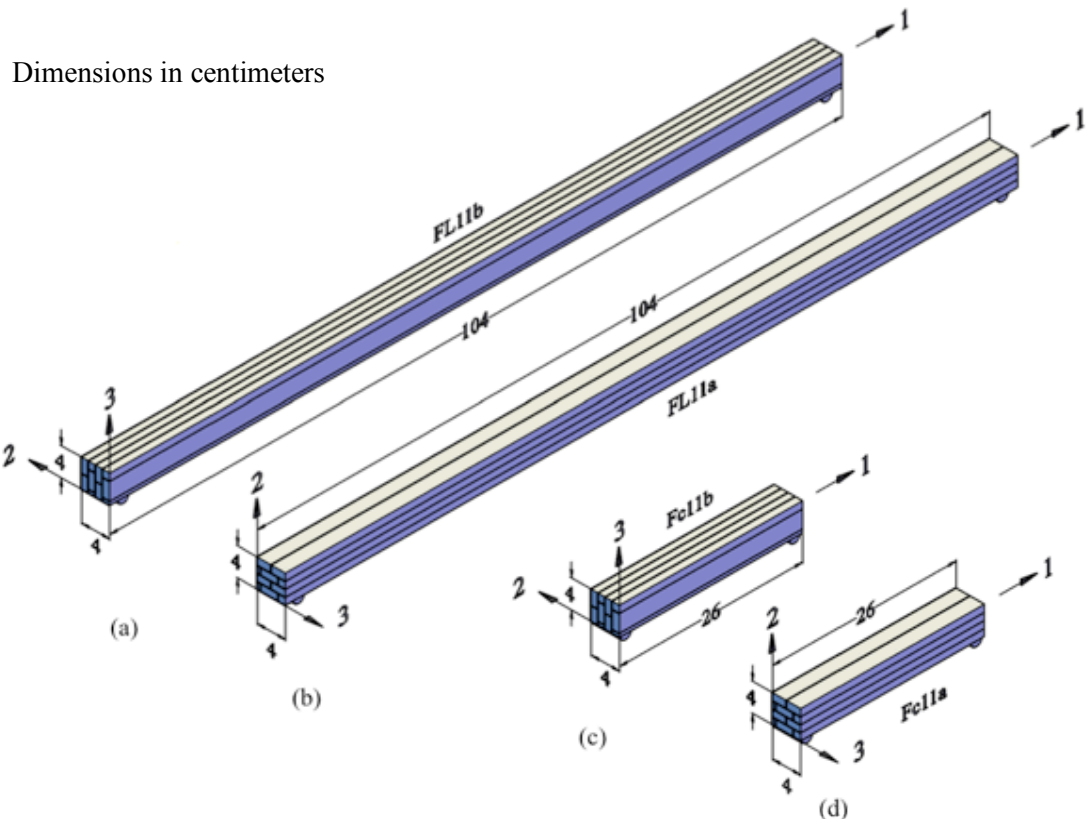
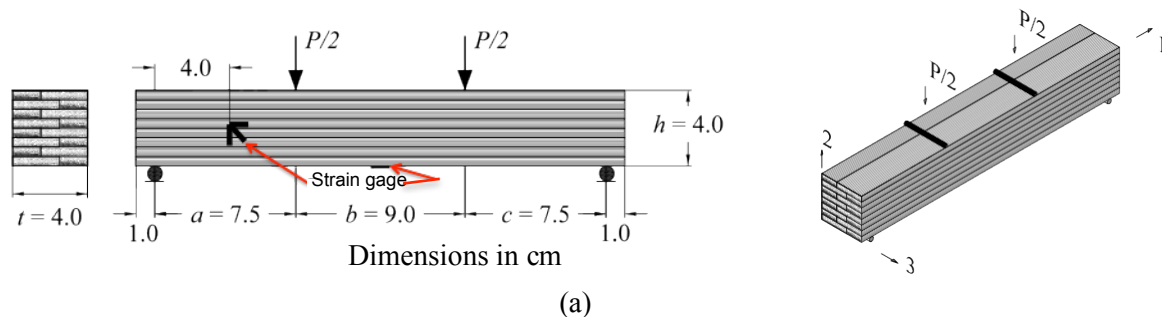


Figure 3. Types of bending samples: (a) FL11b, (b) FL11a, (c) Fc11b y (d) Fc11a.

Bending test of short samples

The short samples were 26cm length and were tested with a span of 24cm, then, the relationship between span and height was 6. The distance b (Figure 4) between the applied loads was 9cm.

The longitudinal strain of all samples was measured using a strain gage located on the lower face and the middle of the span. Additionally, a rectangular rosette was installed on the neutral axis at 4cm from one of the supports, on three samples of each type. Figure 4 shows the assembly for the bending test of short samples. Figure 4(a) corresponds to the samples Fc11a, where the axis 2 is parallel to the load, and Figure 4(b) corresponds to the samples Fc11b with the axis 3 parallel to the load.



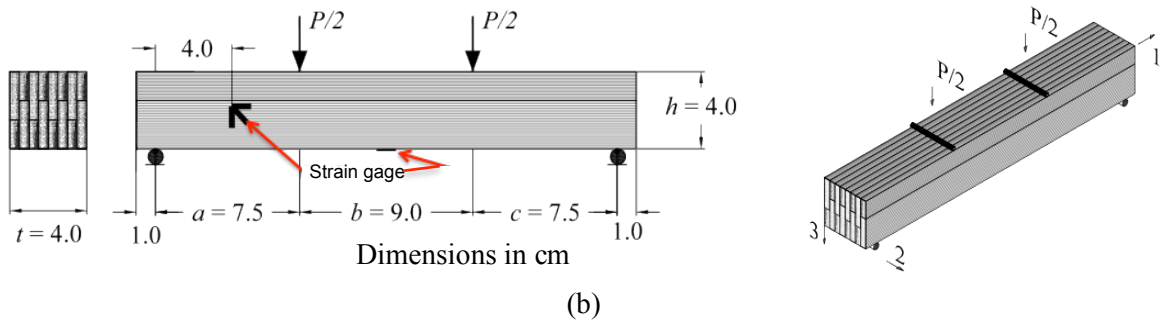


Figure 4. Assembly for tests of short samples: (a) Fc11a y (b) Fc11b.

Bending test of long samples

In order to have a relationship between span and height of 25 to obtain failure by bending, the span in the bending test of long samples was 100cm. The length of the samples was 104cm, considering that the distance of 2cm between the support and the end of the samples would be enough to prevent the sample slipping from the support when it has the deflection corresponding to the maximum load or before.

Two types of long bending samples named FL11a and FL11b were tested. In the samples FL11a, axis 2 is parallel to the load and in the samples FL11b, axis 3 is parallel to the load. A rectangular rosette was installed on the neutral axis at 20cm from one of the supports on three samples of each type. The longitudinal strain was measured using a strain gage and the vertical displacement in the middle of the span was read with a LVDT (Figure 5).

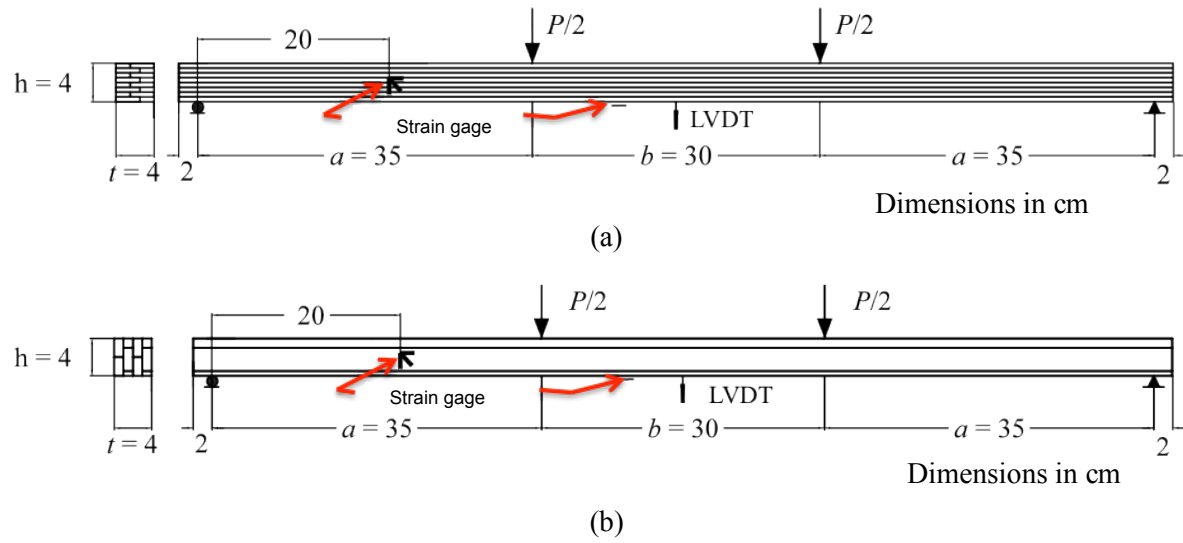


Figure 5. Assembly for test of long samples: (a) FL11a y (b) FL11b.

RESULTS AND DISCUSSION

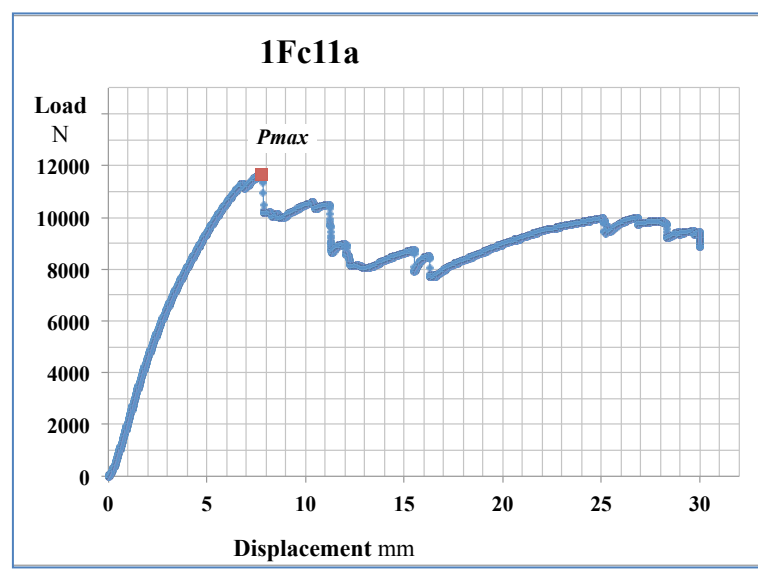
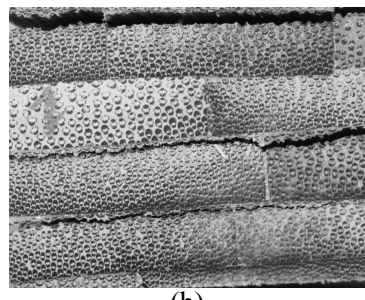
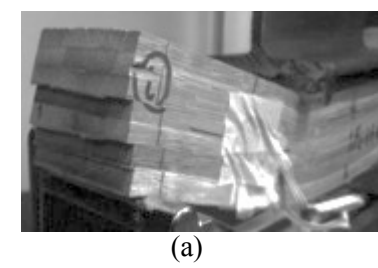
Bending test of short samples

All Fc11a samples had parallel cracks between boards in the extreme thirds near the supports. These fissures represent a shear failure parallel to the fibres. Observing the digital images of the cross section of the samples ends, the failure surface had presented in the board that had less density of fibres in the zone of union. Crushing was observed both in the supports and in the load application points.

The load displacement diagrams of the samples had approximately the same behaviour. The curve grows continuously until it reaches its maximum load, where the first failure surface and loss of resistance were observed. In the discharge zone, the curve jumps when other failure surfaces appeared. Figure 6 shows the final state of sample 1Fc11a and its load displacement diagram.

All Fc11b samples had a crack surface near the neutral plane in each of the extreme thirds of the beam, with the exception of 10Fc11b, which was not tested until the failure. This type of fracture represents a shear failure parallel to the fibre. Additionally, crushing was observed in the supports and load application points.

The load displacement diagrams of Fc11b samples had approximately the same behaviour than Fc11a samples. Figure 7 shows sample 1Fc11b after the appearance of its first crack, and its load displacement diagram.



(c)

Figure 6. 1Fc11a Test: (a) Left side, (b) fissures (c) load displacement diagram.

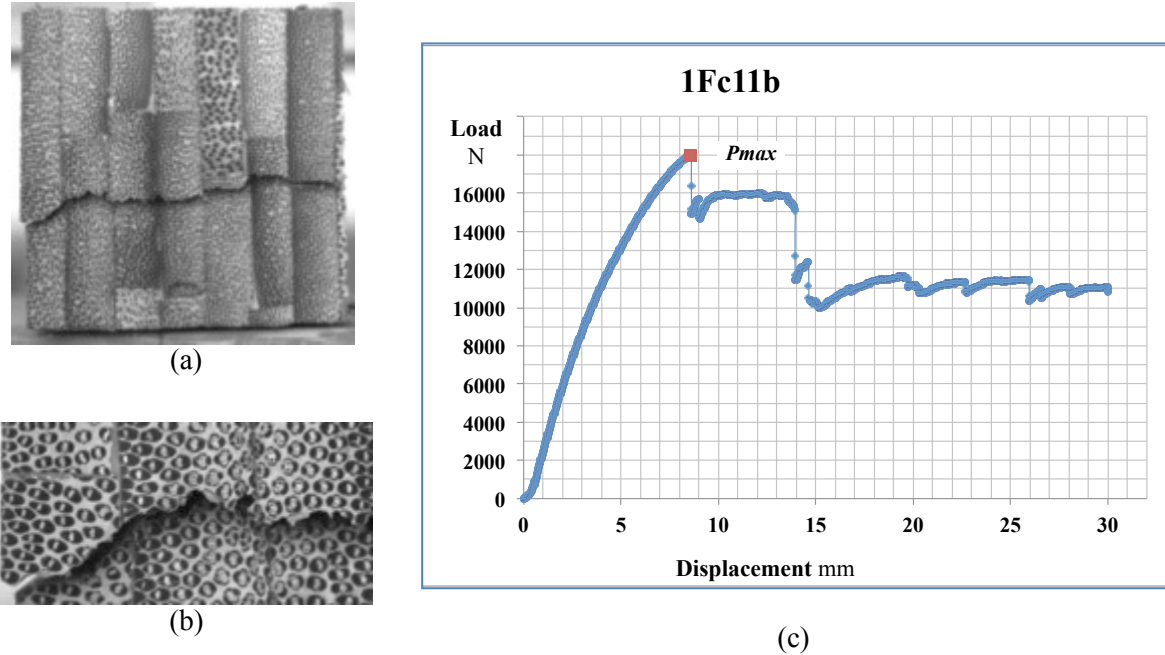


Figure 7. 1Fc11b Test: (a) Left side, (b) approach of fissure (c) load displacement diagram.

Shear Stress

The shear stress was calculated based on Equation 1, where V is the shear in the extreme thirds, P is the applied load, t the thickness and h the height of the cross section. The maximum shear stress was calculated with same equation (1), considering P as the maximum applied load P_{max} .

$$\tau = \frac{3V}{2th} = \frac{3P/2}{2th} \quad (1)$$

Shear modulus

The angular strain was calculated based on Equation (2), where ε_{45° is the strain at 45° , ε_1 is the horizontal strain and ε_2 is the vertical strain.

$$\gamma_{12} = 2\varepsilon_{45^\circ} - \varepsilon_1 - \varepsilon_2 \quad (2)$$

The shear modulus G was calculated as the slope of the linear regression of the stress-strain curve points located between 20% and 75% of the maximum shear stress (Figure 8). The range adopted to calculate the shear modulus was the same adopted to calculate the modulus of elasticity in the bending test of long

samples.

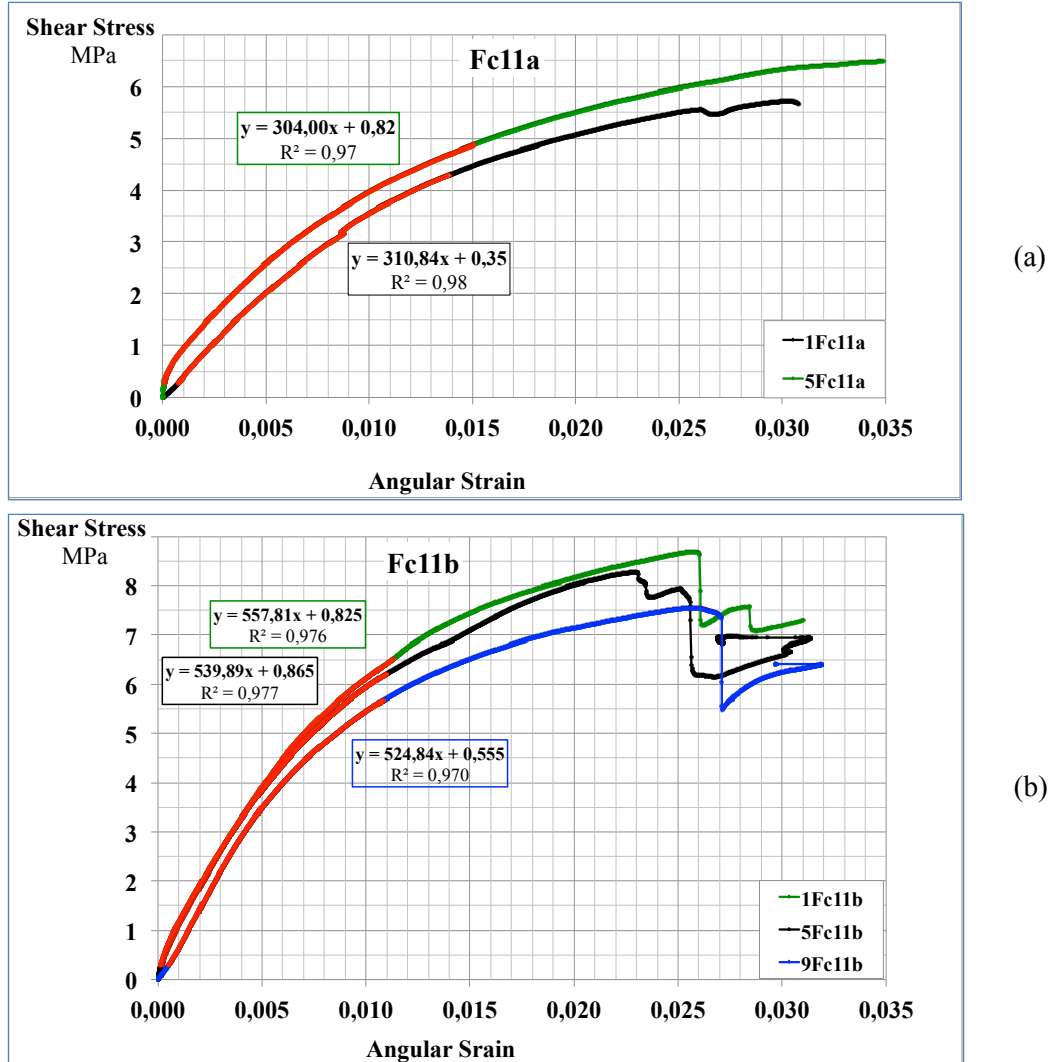


Figure 8. Stress vs. Angular Strain Graphs: (a) Fc11a and (b) Fc11b

The maximum shear stress and the shear modulus determined are shown in Table 1.

Table 1. Maximum Shear Stress. Shear Modulus

FC11a				FC11b			
Specimen	τ_{max} Mpa	G Mpa	Correlation coef	Specimen	τ_{max} Mpa	G Mpa	Correlation coef
1Fc11a	5,72	311	0,9922	1Fc11b	8,69	558	0,9762
2Fc11a	6,50			2Fc11b	8,03		
3Fc11a	5,77			3Fc11b	7,88		
4Fc11a	6,50			4Fc11b	8,88		
5Fc11a	6,50			5Fc11b	8,27		
6Fc11a	6,11			6Fc11b	7,64		
7Fc11a	5,74			7Fc11b	8,44		
8Fc11a	5,85			9Fc11b	7,55		
9Fc11a	6,40			10Fc11b	525		
10Fc11a	6,52						

All samples failed by shear parallel to the fibre. The average value of maximum shear stresses in Fc11a tests was 6.2MPa, with a variation coefficient of 0.06, and 8.2MPa in Fc11b tests, with a variation coefficient of 0.03.

In general, the displacement load curve shapes for the short bending samples were similar: they have an accommodation zone, an elastic and inelastic zone before the maximum load. After reaching the maximum load, the sample continues resisting load.

Bending tests of long samples

FL11a tests show an elastic behaviour followed by an inelastic behaviour before reaching the maximum load. At this time, there is a breakage of the fibres located in the half of the span. Then, the load is reduced gradually. In some samples (2FL11a, 3FL11a, 8FL11b and 10FL11a), the test was stopped due to the high deflections. In others (4FL11a, 5FL11a, 6FL11a, 7FL11a and 9FL11a), after time a shear failure occurred in the extreme thirds. Figure 9 shows the load displacement diagram of 3FL11a and 4FL11a tests. The failure of sample 4FL11a is shown in Figure 10.

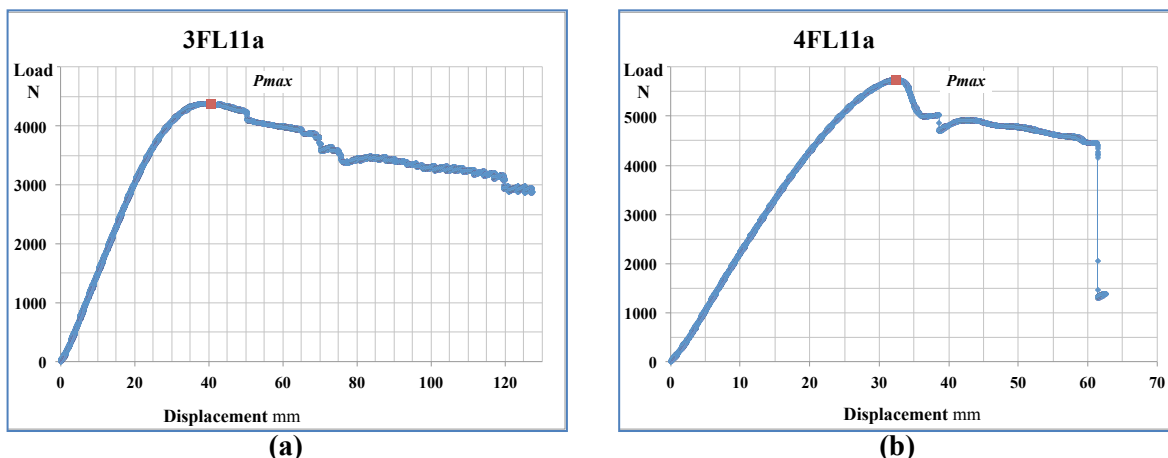


Figure 9. Load Displacement Graph: (a) 3FL11a y (b) 4FL11a



Figure 10. Sample 4FL11a: (a) tension crack and (b) shear failure near the support

In general, the fissures due to tension started in the knots. Crushing at the load application points was observed in all tests.

All the FL11b test samples had fissures due to tension in the lower part (Figure 11).

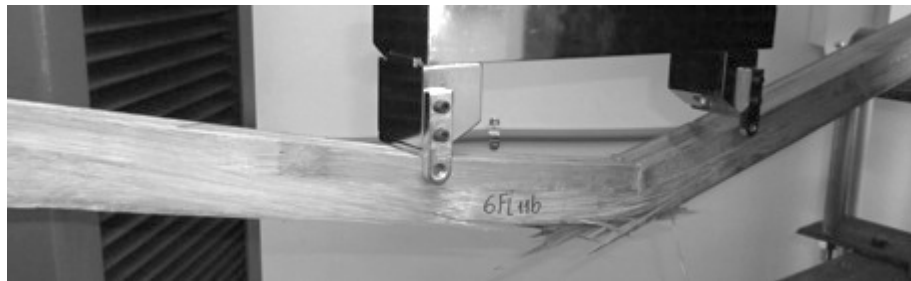


Figure 11. Sample 6FL11b at the end of the test

The load displacement diagrams of the samples had approximately the same behaviour. The curve grows continuously until reaching its maximum load. Then, it loses load gradually until the end of test (Figure 12).

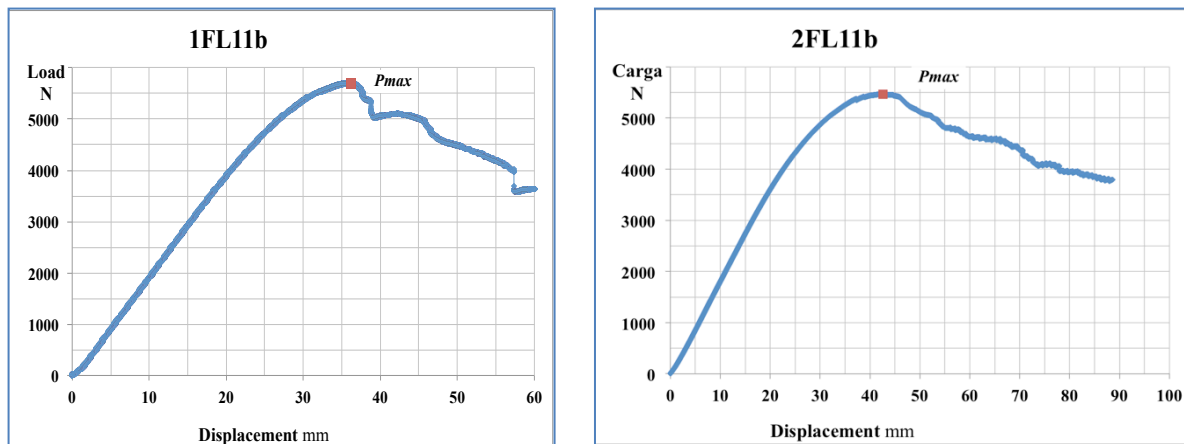


Figure 12. Load Displacement tests: (a) 1FL11b and (b) 2FL11b

Bending stress

The bending stress was calculated based on Equation (3), where M is the moment, S the section modulus, P the applied load and a the horizontal distance between the support and the load. The bending strength was calculated with the same equation, considering M as the maximum moment and P as the maximum applied load.

$$\sigma = \frac{M}{S} = \frac{Pa}{2S} \quad (3)$$

The modulus of elasticity E_1 was calculated as the slope of the linear regression of the stress-strain curve points located between 20% and 75% of the maximum stress (Figure 13). In the ISO 22157 (ISO 2004), for round bamboo, the modulus of elasticity E_1 is calculated as the slope of the stress-strain curve between 10% and 80% of the maximum stress.

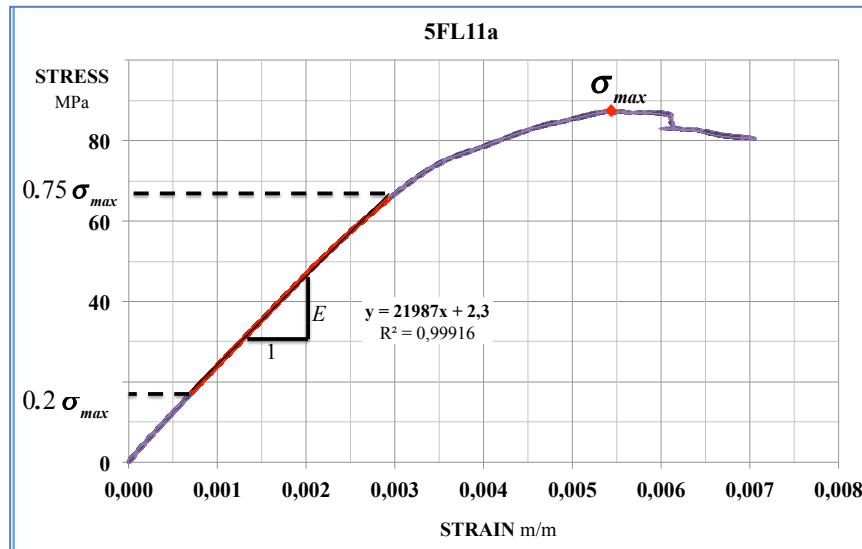


Figure 13. Calculus of the Modulus of Elasticity for 5FL11a Sample

Figure 14 and Figure 15 show the stress-strain curve until reaching the maximum load of the FL11a and FL11b tests, respectively. The major and minor elastic moduli of elasticity are indicated in each graph. In both cases, the curves dispersion in the elastic range was low.

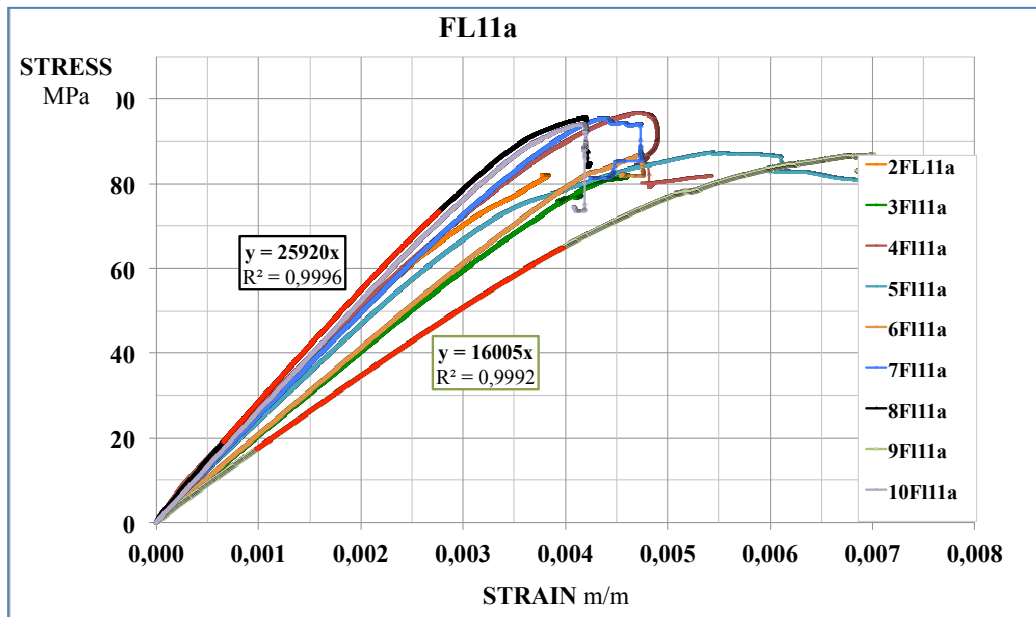


Figure 14. Stress Strain Curves of FL11a Samples

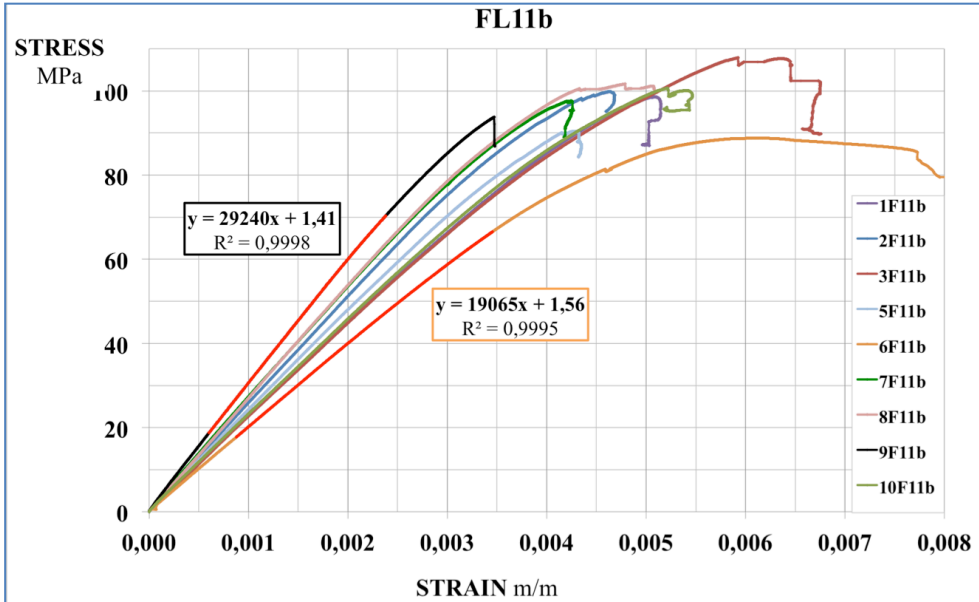


Figure 15. Stress Strain Curves of FL11b Samples

Based on the Equation (4), to calculate the displacement in the centre of the span Δ of a beam with two symmetrical loads ($P/2$), the modulus of elasticity was also determined with the displacement data of the LVDT, using the Equation (5) and considering only the displacement due to bending. In the Equation (5), m is the slope of the linear regression of the points between 20 and 75% of the maximum load and equal to P/Δ ; a is the distance between the support and the point of application of the load; I is the moment of inertia; and L is the span.

$$\Delta = \left(\frac{P}{2} \right) \frac{a}{24EI} (3L^2 - 4a^2) \quad (4)$$

$$E = \frac{m}{2} \frac{a}{24I} (3L^2 - 4a^2) \quad (5)$$

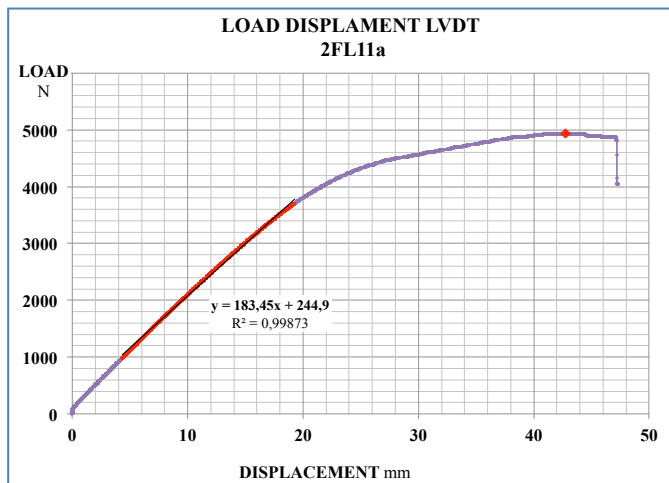


Figure 16. shows the load displacement graph for test 2FL11a elaborated with the displacement data

measured with LVDT.

Figure 16. Load Displacement Curve for 2FL11a Test Using LVDT

Table 2 shows the values of the modulus of elasticity and bending strength, calculated with the equation 3, considering M as the maximum moment and P as the maximum applied load. In FL11a tests, the average value of the bending strength was 93.9MPa with a standard deviation of 6.1MPa and a variation coefficient of 0.06. The average modulus of elasticity calculated with the longitudinal strain readings was 23,050MPa, with a standard deviation of 2337MPa and a variation coefficient of 0.10. The value of the modulus of elasticity of test 9FL11a was not taken into account because it was an outlier according to the Chauvenet exclusion criterion. The average modulus of elasticity calculated with the LVDT displacement readings was 17,159MPa, with a standard deviation of 1059MPa and a variation coefficient of 0.06.

Table 2. Bending strength. Modulus of elasticity

Specimen	Bending strength f_r Mpa	E_1 Strain Mpa	Correlation Coef	E_1 LVDT Mpa	Correlation Coef	Specimen	Bending strength f_r Mpa	E_1 Strain Mpa	Correlation Coef	E_1 LVDT Mpa	Correlation Coef
2FL11a	85,95	24107	0,9998	15530	0,9994	1FL11b	103,18	21421	0,9998	17669	0,9998
3FL11a	86,11	19596	0,9999			2FL11b	104,49	24986	0,9999		
4FL11a	101,11	22889	0,9997	18386	0,9996	3FL11b	112,91	21075	0,9995	17945	0,9995
5FL11a	91,55	21987	0,9996	16698	0,9993	4FL11b	111,01		0,0000		
6FL11a	91,03	20203	0,9999			5FL11b	94,65	23253	0,9999		
7FL11a	99,97	24065	0,9999			6FL11b	92,89	19065	0,9997	17312	0,9995
8FL11a	100,11	25920	0,9998	18106	0,9990	7FL11b	102,16	25879	0,9999	18943	0,9999
9FL11a	90,76	*16005	0,9996	16706	0,9996	8FL11b	106,38	26225	0,9998	19160	0,9998
10FL11a	98,50	25630	0,9999	17526	0,9993	9FL11b	98,18	29240	0,9999	19956	0,9996
						10FL11b	105,41	21925	0,9998		

Excluded

In FL11b tests, the average value of the bending strength was 103.1MPa, with a standard deviation of 6.5MPa and a variation coefficient of 0.06. The average modulus of elasticity calculated with the longitudinal strain readings was 23,674MPa, with a standard deviation of 3,170MPa and a variation coefficient of 0.13. The average modulus of elasticity calculated with the LVDT displacement readings was 18,498MPa, with a standard deviation of 1,016MPa and a variation coefficient of 0.05.

CONCLUSIONS AND RECOMMENDATIONS

The slats (boards) orientation under bending influences their resistance, stiffness and failure. The values of stresses and elastic moduli are higher in samples requested to bending when the normal stresses are perpendicular to the plane of the boards than when they are parallel to them. In the first case, the normal stresses are resisted by alternating zones of low and high density of fibres and, in the second case, by fairly uniform zones of concentration of fibres.

In general, the dispersion of the mechanical response of the tests in LGB samples is low compared with the test in raw bamboo. This indicates that the transformation carried out in the *Guadua* to convert it into LGB homogenizes its physical and mechanical characteristics allowing a greater structural reliability.

The modulus of elasticity calculated using the Stress-Strain graph is higher than the modulus of elasticity calculated with the displacement. In the last case, the displacement due to shear was not taken into account because the relationship of span and height was 25. It is recommendable to study the displacement due to

*

shear, because LGB is a composite material with only longitudinal fibres.

To prevent crushing in the load points steel pads could be used.

It is recommended to change the range adopted for the determination of elastic constants specially for bending in short samples. In this case the upper level is in the yield zone and the estimated shear modulus is not accurate. For bending in long samples the range could be included in the elastic zone but is recommendable that the upper level be lower to guarantee that effectively the range is included in the elastic zone.

REFERENCES

AIS Asociación Colombiana de Ingeniería Sísmica. 2010a. Reglamento Colombiano de Construcción Sismo Resistente.

Correal D, J. F., & Arbeláez C, J. (2010). Influence of Age and Height Position on Colombian *Guadua angustifolia* Bamboo Mechanical Properties. *Maderas. Ciencia Y Tecnología*, 12(2), 105–113.

Correal, J. F., Echeverry, J. S., Ramírez, F., & Yamín, L. E. (2014). Experimental evaluation of physical and mechanical properties of Glued Laminated *Guadua angustifolia* Kunth. *Construction and Building Materials*, 73, 105–112.

Correal, J. F., & Ramírez, F. (2010). Adhesive bond performance in glue line shear and bending for glued laminated guadua bamboo. *Forest Research Institute*, 22(4), 433–439.

Cortés, J. C. (2009). Evaluación de la Influencia del tipo de pegante en el comportamiento mecánico de guadua laminada prensada pegada. Universidad Nacional de Colombia.

Cortés, J. C., Lozano, J., Rusinque, M., & Takeuchi, C. P. (2010). Assessment of the influence of glue type in the mechanical behaviour of glued laminated guadua (bamboo). In 12th International Conference on Non-Conventional Materials and Technologies (IC NOCMAT 2010).

González, H. A., Hellwig, S., & Montoya, J. A. (2008). Resultados del ensayo del modulo de Young y resistencia a la flexión de vigas laminadas de *Guadua angustifolia* Kunth. *Scientia et Technica*, (40), 291–296.

González, H. A., Hellwig, S., & Montoya, J. A. (2008). Comportamiento a la cizalladura de vigas encoladas laminadas de *Guadua angustifolia* Kunth. *Scientia et Technica*, (39), 428–433.

González, J. C., & Leguizamón, Y. (2012). Determinación de la resistencia a compresión paralela a la fibra de la Guadua en función del contenido de humedad. Universidad La Gran Colombia.

González, H. A., Montoya, J. A., & Bedoya, J. R. (2006). Esfuerzo de tensión y la influencia de la humedad relativa del ambiente y la altura a lo largo del tramo en la especie de bambú *Guadua angustifolia* Kunth. *Scientia et Technica*, XII(32), 445–450.

Hackmayer, L. C., Rodríguez, N., & Takeuchi, C. P. (2010). Flexion Behaviour of solid section beams of glued laminated guadua. In IC-NOCMAT 2010. Cairo.

ISO International Organization For Standardization (2004). ISO/DIS- 22157 Determination of physical and mechanical properties of bamboo.

López, L. F., & Correal, J. F. (2009). Estudio exploratorio de los laminados de bambú *Guadua angustifolia* como material estructural. Maderas. Ciencia Y Tecnología, 11(3), 171–182.

Osorio, J. A., Ciro, H. J., & Vélez, J. M. (2005). Influence of physical parameters in the design resistance to compression of the *Guadua angustifolia* Kunth. Dyna, 72, 1–6.

Osorio, J. A., Vélez, J. M., & Ciro, H. J. (2007). Internal structure of the guadua and its incidence in the mechanical properties. Dyna, 74(153), 81–94.

LIST OF FIGURES

Figure 1. Manufacture of LGB blocks

Figure 2. Coordinate system for LGB blocks

Figure 3. Types of bending samples: (a) FL11b, (b) FL11a, (c) Fc11b y (d) Fc11a.

Figure 4. Assembly for tests of short samples: (a) Fc11a y (b) Fc11b.

Figure 5. Assembly for test of long samples: (a) Fl11a y (b) Fl11b.

Figure 6. 1Fc11a Test: (a) Left side, (b) fissures (c) load displacement diagram.

Figure 7. 1Fc11b Test: (a) Left side, (b) approach of fissure (c) load displacement diagram.

Figure 8. Stress vs. Angular Strain Graphs: (a) Fc11a and (b) Fc11b

Figure 9. Load Displacement Graph: (a) 3FL11a y (b) 4FL11a

Figure 10. Sample 4FL11a: (a) tension crack and (b) shear failure near the support

Figure 11. Sample 6FL11b at the end of the test

Figure 12. Load Displacement tests: (a) 1FL11b and (b) 2FL11b

Figure 13. Calculus of the Modulus of Elasticity for 5FL11a Sample

Figure 14. Stress Strain Curves of FL11a Samples

Figure 15. Stress Strain Curves of FL11b Samples

Figure 16. Load Displacement Curve for 2FL11a Test Using LVDT

LIST OF TABLES

Table 1. Maximum Shear Stress. Shear Modulus

Table 2. Bending strength. Modulus of elasticity

